Int. J. Simul. Multidisci. Des. Optim. 16, 28 (2025)

https://doi.org/10.1051/smdo/2025030

IJSMDO

Available online at:
https://www.ijsmdo.org

Research Article

Open Access

Optimal control modelling of XEC SARS-CoV-2 variant with combined ELIXIR-COVID and ADSAK-COVID therapies

Christophe Kikmo Wilba[1,*], Simon Gnassiri[1], Bertin Sone Enone[2], and Njifenjou Abdou[3]

[1] National Advanced School of Engineering, University of Douala, Douala, Cameroon
[2] Department of Pharmaceutical Sciences, Faculty of Medicine and Pharmaceutical Sciences, University of Douala, Douala, Cameroon
[3] Department of Mathematics, National Advanced School of Engineering, University of Yaounde 1, Yaounde, Cameroon

Received: 27 August 2025 / Accepted: 01 October 2025

Abstract. The XEC variant of SARS-CoV-2, first identified in December 2024, exhibits heightened transmissibility and partial vaccine resistance, posing significant public health challenges. We present a nonlinear SEIHRD compartmental model integrating antiviral therapeutics ELIXIR-COVID and ADSAK-COVID, with an optimal control framework to determine dynamic vaccination and treatment strategies that minimize infections, hospitalizations, and deaths under resource constraints. Numerical simulations were calibrated using early outbreak data and epidemiological reports, with parameters drawn from the literature and estimated from analogous variants and regional demographics. Model fitting employed least-squares optimization, ensuring accurate reproduction of epidemic trajectories. Sensitivity analyses assessed robustness to parameter uncertainties. Results demonstrate that combined administration of ELIXIR-COVID and ADSAK-COVID substantially reduces epidemic peaks and mortality, outperforming static or single-intervention strategies. This approach provides a quantitative, contextually adapted decision-support tool for policymakers, facilitating efficient antiviral allocation and vaccination planning, and exemplifies the novel integration of dual-therapy modeling for emerging SARS-CoV-2 variants in resource-limited settings.

Keywords: XEC variant / mathematical modeling / optimal control / antiviral therapy / numerical simulation

1 Introduction

Since its emergence in 2019, SARS-CoV-2 has caused a global pandemic, placing healthcare systems under significant strain and highlighting the urgent need for reliable decision-support tools. The emergence of variants of concern, such as XEC, requires rapid adaptation of health policies, making accurate epidemic forecasting essential. Mathematical epidemiological modeling has proven crucial for guiding strategies, including vaccination and the optimal allocation of therapeutic resources. Most existing models emphasize vaccination and conventional treatments while largely neglecting traditional therapies, which are widely used in Sub-Saharan Africa and other resource-limited regions [1,2]. In particular, ELIXIR-COVID and ADSAK-COVID, developed from local plants by Mgr Samuel Kleda in Cameroon, have demonstrated empirical efficacy. However, their integration into theoretical models remains limited, reducing the applicability of these tools to local contexts where vaccination coverage is partial and adherence to traditional remedies is high [3–7].

To address this gap, we propose a novel framework combining enriched compartmental modeling with optimal control theory, explicitly incorporating the effects of these traditional treatments. This framework quantifies their impact on viral load, hospitalization, and mortality, and simulates optimal administration strategies under logistical constraints. By exploring scenarios that combine vaccination, phytotherapeutic interventions, and preventive measures, we provide a robust, contextually adapted decision-support tool [8–14].

The introduction of optimal control in this context represents a key contribution, offering a quantitative tool to allocate resources effectively while integrating local therapeutic practices. This approach directly addresses gaps in the literature, particularly the lack of models incorporating traditional treatments in regions with partial vaccination coverage.

* e-mail: christophe.kikmo@univ-douala.cm

The article is structured as follows: Section 2 describes the mathematical model; Section 3 presents the optimal control framework; Section 4 details numerical results and simulations; and Section 5 discusses implications, limitations, and future perspectives.

2 Modelling

We consider a compartmental model for the transmission dynamics of the SARS-CoV-2 XEC variant, explicitly integrating the effects of ELIXIR-COVID and ADSAK-COVID treatments. The following assumptions underpin the model and are justified according to epidemiological principles and empirical evidence:

- Imperfect isolation of infected individuals: Isolation of infected individuals is not absolute. Transmission may occur even under strict isolation through indirect contact or contaminated surfaces [15–17]. This is incorporated in the model by a non-zero transmission rate from isolated individuals, reflecting residual viral spread despite containment measures.
- Safe burial practices: Individuals who die outside healthcare facilities are assumed to be buried under controlled conditions, minimizing post-mortem transmission. This is modeled by effectively removing deceased individuals from the transmission chain once proper burial protocols are applied.
- Administration of treatments (ELIXIR-COVID and ADSAK-COVID): Treatments are administered to infected individuals, their close contacts, and high-risk populations. These therapies are assumed to reduce viral load rapidly during early infection stages, thereby lowering both disease severity and secondary transmission. The effect is incorporated via a reduction in the infectiousness parameter for treated individuals.
- Efficacy of treatments: Both therapies are assumed to reduce viral load, hospitalizations, and the need for oxygen supplementation, consistent with documented clinical observations [18–20]. Treatment efficacy is modeled as a function decreasing the probability of onward transmission and accelerating recovery.
- Vaccination as a complementary control: Vaccination is incorporated as a separate control variable in the model, interacting with treatment effects. It reduces susceptibility among vaccinated individuals and complements the therapeutic interventions, consistent with optimal control strategies.
- Variant-specific characteristics: The XEC variant is assumed to have enhanced transmissibility and potential partial resistance to conventional treatments. The model accounts for differential transmission rates among susceptible, infected, and treated individuals.
- Temporal dynamics of infection and treatment: Treatment effects are most pronounced when administered early in the course of infection. The model represents this by a time-dependent efficacy function that decreases as the infection progresses, reflecting reduced therapeutic impact at later stages.
- Behavioral factors: Individuals receiving treatments are assumed to adhere to preventive measures, including self-isolation, hand hygiene, and social distancing. These behaviors further reduce transmission probability and are incorporated into the effective contact rate of treated individuals.

Justification of functional forms:

- Transmission is modeled using standard mass-action incidence, reflecting contacts between susceptible and infectious individuals.
- Treatment effects are represented as multiplicative reductions in infectiousness and progression rates, consistent with observed viral kinetics.
- Vaccination is incorporated via a susceptibility reduction term, allowing integration with the control framework.

These assumptions provide a mathematically tractable yet epidemiologically realistic framework for studying the combined effects of vaccination and traditional therapies in controlling the XEC variant.

2.1 Study of model variables

Mathematical modelling endeavors to classify individuals into distinct compartments to assess the spread of the SARS-CoV-2 XEC variant and the effects of ELIXIR-COVID and ADSAK-COVID treatments. Each compartment represents a specific demographic or epidemiological stratum within the population, sampled at discrete times, often resulting in markedly different dynamics [21–24].

We define the following variables for the compartmental model:

- $S(t)$: People vulnerable extremely to contracting disease. Hospital staff and carers of infected patients alongside their relatives are included in this diverse group quite broadly. Taking ELIXIR-COVID and ADSAK-COVID modifies exposure for individuals at high risk of infection quite substantially every day. Likelihood of infection depends heavily on myriad social interactions and prevention measures put firmly in place by professionals.
- $E(t)$: People harboring somewhat virulent infections displaying moderately severe symptoms of disease. Infected individuals exhibiting rather moderate symptoms are typically associated with a relatively less severe form of SARS-CoV-2 infection evidently. Symptoms manifest as moderately high fever and dry cough alongside fatigue headache loss of appetite and muscular aches quite frequently. These individuals can still transmit virus with considerably lower viral load than those in next group $I(t)$.
- $I(t)$: People with a severe form of disease exhibit persistent high fever trouble breathing chest pain mental confusion bluish skin coloration and severe oxygen deficiency. These folks require immediate medical attention often in ICU and pose high risk of transmitting virus rapidly among others nearby.
- $H(t)$: Patients requiring medical attention are frequently hospitalized or kept in isolation pending diagnosis and subsequently subjected to rigorous treatment protocols. Individuals hospitalized owing largely to marked deterioration in condition are encompassed within this

particular category. These individuals get treated in intensive care units or get isolated pretty quickly in various care centers rather haphazardly as isolation prevents transmission. ELIXIR-COVID and ADSAK-COVID treatments might be administered quite possibly reducing severity of infection or risk of various nasty complications.
- D(t): People who've fallen prey to COVID-19 suddenly. Individuals who fell prey to SARS-CoV-2 without receiving either ELIXIR-COVID treatment or some ADSAK-COVID therapy are part of this group. Most fatalities likely occur in classes E(t) and I(t) characterized by woefully limited access to marginally effective treatment somehow.
- R(t): People who've recovered successfully from infection. ELIXIR-COVID treatment recipients and ADSAK-COVID patients exhibiting partial or full immunity contingent upon successful treatment efficacy and initial viral loads demonstrated a positive response. People within this demographic have largely lost capacity for spreading disease further quite rapidly now.
- Total Population N(t): The total population at time t is the sum of all the classes: $N(t) = S(t) + E(t) + I(t) + H(t) + D(t) + R(t)$.
- Living Population Nv(t): The living population at time t is defined as the sum of susceptible, infected, hospitalized and cured individuals, excluding deaths: $Nv(t) = S(t) + E(t) + I(t) + H(t) + R(t)$.

2.2 Effects of treatments and vaccination

Model incorporates effects of ELIXIR-COVID and ADSAK-COVID treatments hypothesizing reduction in transition rate between classes E(t) and I(t) and mortality rate D(t) significantly. These treatments may hasten recovery thereby swelling ranks of R(t) class.

Incorporation of vaccination as means for controlling situation presents potential avenue for investigation within target population under specific policy implementations.

SARS-CoV-2 virus XEC variant propagation gets investigated thoroughly under mathematical model consideration alongside ELIXIR-COVID and ADSAK-COVID therapeutic interventions impact. Population at risk stays constant presumably because new individuals recklessly flow in at rate β owing largely to births or mobility. A certain degree of susceptibility denoted as S(t) is expected among this motley crew of individuals prone to infection.

The investigation focuses on the dynamics of susceptibility S(t), which is defined as the probability of an individual becoming infected.

Susceptible individuals can contract disease in various weird ways namely as follows pretty much somehow under certain conditions:
- By making physical contact with individuals in class E(t) (moderate infectees): Susceptible individuals can become infected at a rate β_0 by making physical contact with individuals in class E(t).
- By making physical contact with individuals in class I(t) (severe infectees): Susceptible individuals can also become infected by making physical contact with individuals in class I(t).
- By making physical contact with individuals who are isolated with the infection: Some people are isolated due to the severity of their symptoms, but their isolation isn't perfect, and $1-\sigma_1$ of them can still transmit the virus at a $\delta\beta_0$ rate.
- Transmission can also occur through contact with the bodies of deceased individuals when traditional rituals are performed before burial. The disease is believed to be transmitted by these individuals at a rate $\beta_0\nu_2$, contingent on the proportion $1-\sigma_2$ of the deceased individuals involved.

2.3 Transmission and progression of infected individuals

Moderately Infected E(t)

A proportion p of infected individuals develop mild symptoms, while others show more severe symptoms. Individuals in class E(t) can progress in different ways:
- Cure naturally through the immune system at a rate γ_E without requiring medical attention.
- Die as a result of the disease at a rate δ_E.
- Be hospitalized at a rate η_E.
- Progress to more severe symptoms at a rate α.

Severely Infected I(t)

Individuals in class I(t), due to the severity of their symptoms, generally cannot recover without treatment. They may:
- Die as a result of the disease at a rate δ_I.
- Go to treatment centers to receive care at a rate η_I.

Hospitalized Individuals H(t)

Individuals hospitalized may recover at a rate γ_H or die at a rate δ_H depending on the effectiveness of the care received.

Mortality and Recruitment

Natural mortality affects the living population, excluding deaths due to COVID-19, at a constant rate μ. The living population Nv(t) is thus affected by this natural mortality in addition to the mortality specific to COVID-19.

Transmission Scheme

A set of differential equations governs intricate interactions among various demographic categories including susceptible moderately infected severely infected hospitalized deceased and recovered. Transitions between categories unfold according largely to rates of transmission recovery hospitalization death and efficacy of treatment subsequently. Transmission diagrams offer somewhat obscure visual representations of flows between categories often beneath murky layers of abstraction. Model parameters are painstakingly detailed in Table 1 with each transition rate rigorously defined thereby facilitating thorough understanding of model functionality. Parameters outlined here include several key facets somehow:

Table 1. Parameters of the model and their definitions.

Parameters	Epidemiological analysis	Units
Λ	Recruiting susceptible	Day^{-1}
$\beta_0,\beta_0\alpha_1,\beta_0\alpha_2$	Rate of transmission between the classes	–
δ	Proportion of isolated cases who are still capable of transmission	–
σ_1,σ_2	Proportion of deceased and isolated infected involved in transmitting	–
$\gamma_E,\delta_E,\eta_E,\alpha$	In people with moderate infection, rates of cure, death, hospitalization and progression to severe symptoms	Day^{-1}
γ_H,δ_H	Recovering and dying in hospital	Day^{-1}
μ	Living population natural death rate	Day^{-1}
θ	Proportion of vaccine recipients who develop immunity	–

The model is illustrated by the compartmental diagram shown in Figure 1.

The model resulting from all this is given by:

$$\begin{cases} \dot{S}(t)=\Lambda-\beta_0(1-\theta v)S(t)[E(t)+\delta(1-\sigma_1)H(t)+\alpha_1 I(t)+\alpha_2(1-\sigma_2)D(t)]-(\theta v+\mu)S(t) \\ \dot{E}(t)=p\beta_0(1-\theta v)S(t)[E(t)+\delta(1-\sigma_1)H(t)+\alpha_1 I(t)+\alpha_2(1-\sigma_2)D(t)]-\varphi_1 S(t) \\ \dot{I}(t)=(1-p)\beta_0(1-\theta v)S(t)[E(t)+\delta(1-\sigma_1)H(t)+\alpha_1 I(t)+\alpha_2(1-\sigma_2)D(t)]+\alpha E(t)-\varphi_2 S(t) \\ \dot{H}(t)=\eta_E E(t)+\eta_I I(t)-\varphi_3 H(t) \\ \dot{D}(t)=(\mu+\delta_E)E(t)+(\mu+\delta_I)I(t)-qD(t) \\ \dot{R}(t)=\theta v S(t)+\gamma_E E(t)+\gamma_H H(t)-\mu R(t) \end{cases} \tag{1}$$

$$\text{with}\begin{cases} \varphi_1=(\alpha+\gamma_E+\mu+\delta_E+\eta_E) \\ \varphi_2=(\delta_I+\eta_I+\mu) \\ \varphi_3=(\gamma_H+\delta_H+\mu) \\ \beta=\beta_0(1-\theta v). \end{cases}$$

Model usage reveals pandemic shifts under varied scenarios especially with ELIXIR-COVID and ADSAK-COVID treatments unfolding rapidly across affected populations somehow.

3 Analysis

3.1 Positivity and boundedness

Proposition 1

The positive orthant R_+^6 is positively invariant by the flow of (1). Specifically, if $S(0)>0$, $E(0)\geq 0$, $I(0)\geq 0$, $H(0)\geq 0$, $D(0)\geq 0$, $R(0)\geq 0$, then, $\forall\, t\geq 0$, $S(t)>0$, $E(t)\geq 0$, $I(t)\geq 0$, $H(t)\geq 0$, $D(t)\geq 0$, $R(t)\geq 0$.

Proof

The above proposition will be proved using the theory of monotone systems on the one hand and the comparison principle on the other. In order to establish the aforementioned proposition, it is necessary to demonstrate that, if $S(0)>0$, then $\forall t\geq 0$, $S(t)>0$. The following argument is thus proposed.

$$f(t)=\beta_0(1-\theta v)(E(t)+\delta(1-\sigma_1)H(t)+\alpha_1 I(t)+\alpha_2(1-\sigma_2)D(t))-(\theta v+\mu).$$

Integration of the first equation in (1) from 0 to t ($t>0$) yields

$$S(t)=S(0)\exp\left(\int_0^t -f(s)ds\right)+\exp\left(\int_0^t -f(s)ds\right)\times\int_0^t \Lambda\exp\left(\int_0^u -f(v)dv\right)du.$$

Thus $S(t)>0$, $\forall t\geq 0$.

In order to demonstrate that $E(t)\geq 0, I(t)\geq 0, H(t)\geq 0, D(t)\geq 0, R(t)\geq 0$ for all $t\geq 0$, it is necessary to define the function $g(t)$ such that $(0)\geq 0$, $I(0)\geq 0$, $H(0)\geq 0$, $D(0)\geq 0$ and $R(0)\geq 0$. In order to establish the function $g(t)$, the following definition is proposed:

$$\dot{g}(t)=\theta v S(t)+\gamma_E E(t)+\gamma_H H(t)-\mu g(t).$$

Now consider this system:

$$\begin{cases} \dot{E}(t)=p\beta_0(1-\theta v)S(t)[E(t)+\delta(1-\sigma_1)H(t)+\alpha_1 I(t)+\alpha_2(1-\sigma_2)D(t)]-\varphi_1 S(t) \\ \dot{I}(t)=(1-p)\beta_0(1-\theta v)S(t)[E(t)+\delta(1-\sigma_1)H(t)+\alpha_1 I(t)+\alpha_2(1-\sigma_2)D(t)]+\alpha E(t)-\varphi_2 S(t) \\ \dot{H}(t)=\eta_E E(t)+\eta_I I(t)-\varphi_3 H(t) \\ \dot{D}(t)=(\mu+\delta_E)E(t)+(\mu+\delta_I)I(t)-qD(t) \\ \dot{g}(t)=\theta v S(t)+\gamma_E E(t)+\gamma_H H(t)-\mu g(t). \end{cases} \tag{2}$$

The system of differential equations (2) can be expressed as follows: $\dot{X}(t)=MX(t)$

$$\text{With } X(t)=\begin{pmatrix} E(t) \\ I(t) \\ H(t) \\ D(t) \\ g(t) \end{pmatrix}$$

$$\text{and } M=\begin{pmatrix} p\beta S-\varphi_1 & p\beta\alpha_1 S & p\beta\delta(1-\sigma_1)S & p\beta\alpha_2(1-\sigma_2)S & 0 \\ (1-p)\beta S+\alpha & (1-p)\beta\alpha_1 S-\varphi_2 & (1-p)\beta\delta(1-\sigma_1)S & (1-p)\beta\alpha_2(1-\sigma_2)S & 0 \\ \eta_E & \eta_I & -\varphi_3 & 0 & 0 \\ \mu+\delta_E & \mu+\delta_I & 0 & -q & 0 \\ \gamma_E & 0 & \gamma_H & 0 & -\mu \end{pmatrix}.$$

It can be demonstrated that M is a stable Metzler matrix, and thus the system $\dot{X}(t)=MX(t)$ is a monotone system. It can be concluded that $\mathbb{R}_+^5$ is an invariant by the flow of the system $\dot{X}(t)=MX(t)$. Consequently, it can be deduced that $E(t)\geq 0$, $I(t)\geq 0$, $H(t)\geq 0$, $D(t)\geq 0$, and $g(t)\geq 0$, $\forall t\geq 0$. Furthermore, an application of the comparison theorem [3,4] yields $R(t)\geq g(t)$, $\forall t\geq 0$. Therefore, $R(t)\geq 0$, $\forall\, t\geq 0$.

Proposition 2

It is assumed that the initial conditions of System (1) are those stipulated in Proposition 1.

If $S(0) \le \frac{\Lambda}{(\theta v+\mu)}$, $Nv(0) \le \frac{\Lambda}{\mu}$ and $D(0) \le \frac{\Lambda(\delta_E+\delta_I+2\mu)}{q\mu}$ then $\forall t>0$, $S(t) \le \frac{\Lambda}{(\theta v+\mu)}$, $Nv(t) \le \frac{\Lambda}{\mu}$, $D(t) \le \frac{\Lambda(\delta_E+\delta_I+2\mu)}{q\mu}$ and $N(t) \le \frac{\Lambda(\delta_E+\delta_I+2\mu+q)}{q\mu}$.

Proof

The differential equations describing the dynamics of S(t), Nv(t), and D(t). These equations generally look like this:

$\dot{S}(t) \le \Lambda - (\theta v+\mu)S(t)$, $\dot{Nv}(t) \le \Lambda - \mu Na(t)$, $\dot{D}(t) \le (\mu+\delta_E)E(t) + (\mu+\delta_I)I(t) - qD(t)$.

Applying the method of separation of variables, together with Gronwall's lemma to the above differential inequalities, leads to the following conclusion:

$\dot{S}(t) \le \Lambda - (\theta v+\mu)S(t) \Rightarrow S(t) \le \frac{\Lambda}{(\theta v+\mu)} - \left(S(0) - \frac{\Lambda}{(\theta v+\mu)}\right) e^{-(\theta v+\mu)t}$, thus, $S(t) \le \frac{\Lambda}{(\theta v+\mu)}$ when $S(0) \le \frac{\Lambda}{(\theta v+\mu)}$.

Moreover $\dot{Nv}(t) \le \Lambda - \mu Nv(t) \Rightarrow Nv(t) \le \frac{\Lambda}{\mu} + \left(Nv(0) - \frac{\Lambda}{\mu}\right) e^{-\mu t}$, thus, $Nv(t) \le \frac{\Lambda}{\mu}$ when $Nv(0) \le \frac{\Lambda}{\mu}$. since $Nv(t) \le \frac{\Lambda}{\mu}$ then $E(t) \le \frac{\Lambda}{\mu}$ and $I(t) \le \frac{\Lambda}{\mu}$.

We have: $\dot{D}(t) \le (\mu+\delta_E)\frac{\Lambda}{\mu} + (\mu+\delta_I)\frac{\Lambda}{\mu} - qD(t)$.

$\Rightarrow D(t) \le \frac{\Lambda(\delta_E+\delta_I+2\mu)}{q\mu} + \left(D(0) - \frac{\Lambda(\delta_E+\delta_I+2\mu)}{q\mu}\right)e^{-qt}$

$\Rightarrow D(t) \le \frac{\Lambda(\delta_E+\delta_I+2\mu)}{q\mu}$ when $D(0) \le \frac{\Lambda(\delta_E+\delta_I+2\mu)}{q\mu}$.

Since $N(t) = Nv(t) + D(t)$, $\Rightarrow N(t) \le \frac{\Lambda(\delta_E+\delta_I+2\mu+q)}{q\mu}$.

Thus, the COVID-19 model presented in (1) is mathematically and epidemiologically meaningful, in the feasibility zone $\Omega \subset \mathbb{R}_+^6$ such that

$$\Omega = \left\{(S(t),E(t),I(t),H(t),D(t),R(t)) \in \mathbb{R}_+^6 / S(t) \le \frac{\Lambda}{(\theta v+\mu)}, Nv(t) \le \frac{\Lambda}{\mu} \text{et } D(t) \le \frac{\Lambda(\delta_E+\delta_I+2\mu)}{q\mu}\right\}.$$

3.2 Existing and stable equilibrium without COVID (CFE)

The disease-free equilibrium state, denoted by E_0, is obtained by cancelling the right-hand side of all the equations of the system (1) as well as the variables E, I, H. This equilibrium is referred to as the "COVID-free equilibrium" (CFE). The CFE is defined as follows: $E_0 = (S^*, E^*, I^*, H^*, D^*, R^*)$, where $E^* = I^* = H^* = 0$.

$$\begin{cases} 0 = \Lambda - \beta_0(1-\theta v)S^*(t)[E^*(t) + \delta(1-\sigma_1)H^*(t) + \alpha_1 I^*(t) + \alpha_2(1-\sigma_2)D^*(t)] - (\theta v+\mu)S^*(t) \\ 0 = p\beta_0(1-\theta v)S^*(t)[E^*(t) + \delta(1-\sigma_1)H^*(t) + \alpha_1 I^*(t) + \alpha_2(1-\sigma_2)D^*(t)] - \varphi_1 S^*(t) \\ 0 = (1-p)\beta_0(1-\theta v)S^*(t)[E^*(t) + \delta(1-\sigma_1)H^*(t) + \alpha_1 I^*(t) + \alpha_2(1-\sigma_2)D^*(t)] + \alpha E^*(t) - \varphi_2 S^*(t) \\ 0 = \eta_E E^*(t) + \eta_I I^*(t) - \varphi_3 H^*(t) \\ 0 = (\mu+\delta_E)E^*(t) + (\mu+\delta_I)I^*(t) - qD^*(t) \\ 0 = \theta v S^*(t) + \gamma_E E^*(t) + \gamma_H H^*(t) - \mu R^*(t). \end{cases} \tag{3}$$

Assuming that S^* is greater than or equal to zero, the following equation can be derived from the reorganisation of the system:

$$\begin{cases} \beta[E^* + \delta(1-\sigma_1)H^* + \alpha_1 I^* + \alpha_2(1-\sigma_2)D^*] - (\theta v+\mu) = \frac{\Lambda}{S^*} \\ \beta S^*[E^* + \delta(1-\sigma_1)H^* + \alpha_1 I^* + \alpha_2(1-\sigma_2)D^*] = \frac{\varphi_1 E^*}{p} = \frac{\varphi_2 I^* - \alpha E^*}{1-p} \\ H^* = \frac{\eta_E E^* + \eta_I I^*}{\varphi_3} \\ D^* = \frac{(\mu+\delta_E)E^* + (\mu+\delta_I)I^*}{q} \\ R^* = \frac{\theta v S^* + \gamma_E E^* + \gamma_H H^*}{\mu}. \end{cases}$$

The substitution of the expressions found for H^*, D^*, and R^* in the remaining equations results in a complete expression for the variables S^*, E^*, I^*, H^*, D^*, and R^*.

$$E^* = \frac{p\varphi_2}{(1-p)\varphi_1+\alpha p}I^*,\ H^* = \left(\frac{\eta_E p\varphi_2}{\varphi_3((1-p)\varphi_1+\alpha p)} + \frac{\eta_I}{\varphi_3}\right)I^*,\ D^* = \left(\frac{(\mu+\delta_E)p\varphi_2}{q((1-p)\varphi_1+\alpha p)} + \frac{(\mu+\delta_I)}{q}\right)I^*,$$

$$S^* = \frac{\Lambda}{(\theta v+\mu)} - \frac{\varphi_1\varphi_2}{((1-p)\varphi_1+\alpha p)(\theta v+\mu)}I^*.$$

The replacement of the expressions in question with I^* for the equilibrium model variables in the equation is to be undertaken.

$0 = \Lambda - \beta_0(1-\theta v)S^*(t)[E^*(t) + \delta(1-\sigma_1)H^*(t) + \alpha_1 I^*(t) + \alpha_2(1-\sigma_2)D^*(t)] - (\theta v+\mu)S^*(t)$, Posing $k_1 = \frac{p\varphi_2}{(1-p)\varphi_1+\alpha p}$, $k_2 = \frac{\eta_E p\varphi_2}{\varphi_3((1-p)\varphi_1+\alpha p)} + \frac{\eta_I}{\varphi_3}$, $k_3 = \frac{(\mu+\delta_E)p\varphi_2}{q((1-p)\varphi_1+\alpha p)} + \frac{(\mu+\delta_I)}{q}$

$k_4 = \frac{-\varphi_1\varphi_2}{((1-p)\varphi_1+\alpha p)(\theta v+\mu)}$, that we can get:

$$\left(-\beta\left(\frac{\Lambda}{(\theta v+\mu)} + k_4 I^*\right)(k_1 + \delta(1-\sigma_1)k_2 + \alpha_1 + \alpha_2(1-\sigma_2)k_3) - k_4(\theta v+\mu)\right)I^* = 0$$

So $I^* = 0$, where

$$\left(-\beta\left(\frac{\Lambda}{(\theta v+\mu)} + k_4 I^*\right)(k_1 + \delta(1-\sigma_1)k_2 + \alpha_1 + \alpha_2(1-\sigma_2)k_3) - k_4(\theta v+\mu)\right) = 0.$$

This means $I^* = \frac{(\theta v+\mu)}{\beta(k_1+\delta(1-\sigma_1)k_2+\alpha_1+\alpha_2(1-\sigma_2)k_3)} \times (R_{0c}-1)$ with

$$R_{0c} = \frac{\beta(1-p)\varphi_1 + \alpha p)(k_1 + \delta(1-\sigma_1)k_2 + \alpha_1 + \alpha_2(1-\sigma_2)k_3)}{\varphi_1\varphi_2(\theta v+\mu)}.$$

In this section, the controlled reproduction number R_{0c} is defined as a critical parameter for assessing the impact of ELIXIR-COVID and ADSAK-COVID treatments on the transmission dynamics of the XEC SARS-CoV-2 variant. R_{0c} quantifies viral transmissibility while incorporating the mitigating effects of the treatments on infection spread and severity. When $R_{0c} < 1$, the system reaches a virus-free equilibrium (CFE) $E_0 = \left(\frac{\Lambda}{(\theta v+\mu)}, 0, 0, 0, 0, \frac{\Lambda\theta v}{\mu(\theta v+\mu)}\right)$, indicating that the virus is effectively controlled. Conversely, if $R_{0c} > 1$, the model exhibits two equilibria: the CFE and an endemic equilibrium. In this scenario, the virus persists at a stable but manageable level, reflecting partial containment under treatment interventions.

3.3 Investigate the CFE's overall stability

The objective of this section is to establish the global stability of the virus-free equilibrium E_0 (CFE). This is done by evaluating the effects of two antiviral treatments, ELIXIR-COVID and ADSAK-COVID, on the spread of the XEC SARS-CoV-2 variant. The study hypothesizes that the virus can be fully controlled if these treatments are appropriately administered. Using a Lyapunov function tailored to the model, we analyze the convergence of trajectories toward E_0, ensuring viral elimination under the condition $R_{0c} \le 1$ [8,13,21]. This result confirms the efficacy of ELIXIR-COVID and ADSAK-COVID in containing the epidemic and eradicating the virus from the population.

Proposition 3

The equilibrium point without COVID (CFE) E_0 of the model is globally asymptotically stable if and only if $R_{0c} \le 1$, but unstable if $R_{0c} > 1$.

Proof

To prove this proposition, we assume the following Lyapunov function:

$V(t) = b_1 E(t) + b_2 I(t) + b_3 H(t) + b_4 D(t) + b_5 R(t)$

where b_i, for $i = 1, 2, 3, 4, 5$, are positive constants to be chosen later.

Deriving the derivative of $V(t)$ along the solutions of system (1) with respect to t, we obtain:

$$\frac{dV(t)}{dt} = b_1 \frac{dE(t)}{dt} + b_2 \frac{dI(t)}{dt} + b_3 \frac{dH(t)}{dt} + b_4 \frac{dD(t)}{dt} + b_5 \frac{dR(t)}{dt}$$

$$\begin{aligned}
&= b_1(\beta S(t)[E(t) + \delta(1-\sigma_1)H(t) + \alpha_1 I(t) + \alpha_2(1-\sigma_2)D(t)] - \varphi_1 S(t)) \\
&+ b_2((1-p)\beta_0(1-\theta v)S(t)[E(t) + \delta(1-\sigma_1)H(t) + \alpha_1 I(t) + \alpha_2(1-\sigma_2)D(t)] + \alpha E(t) - \varphi_2 S(t)) \\
&+ b_3(\eta_E E(t) + \eta_I I(t) - \varphi_3 H(t)) + b_4((\mu + \delta_E)E(t) + (\mu + \delta_I)I(t) - qD(t)) \\
&+ b_5(\theta v S(t) + \gamma_E E(t) + \gamma_H H(t) - \mu R(t)).
\end{aligned}$$

Since to $S(t) \le \frac{\Lambda}{(\theta v + \mu)}$ for all $t > 0$, each term can be bounded accordingly.

$$\begin{aligned}
\frac{dV(t)}{dt} &\le b_1\left(\beta \frac{\Lambda}{(\theta v + \mu)}[E(t) + \delta(1-\sigma_1)H(t) + \alpha_1 I(t) + \alpha_2(1-\sigma_2)D(t)] - \varphi_1 \frac{\Lambda}{(\theta v + \mu)}\right) + \\
& b_2\left((1-p)\beta_0(1-\theta v)\frac{\Lambda}{(\theta v + \mu)}[E(t) + \delta(1-\sigma_1)H(t) + \alpha_1 I(t) + \alpha_2(1-\sigma_2)D(t)] + \alpha E(t) - \varphi_2 \frac{\Lambda}{(\theta v + \mu)}\right) + \\
& b_3(\eta_E E(t) + \eta_I I(t) - \varphi_3 H(t)) + b_4((\mu + \delta_E)E(t) + (\mu + \delta_I)I(t) - qD(t)) + \\
& b_5\left(\theta v \frac{\Lambda}{(\theta v + \mu)} + \gamma_E E(t) + \gamma_H H(t) - \mu R(t)\right).
\end{aligned}$$

$$\begin{aligned}
&\le \frac{\left(\alpha_1 b_1 - \alpha_1 b_2(1-p)\beta_0(1-\theta v)\frac{\Lambda}{(\theta v + \mu)} + b_3\eta_I + b_4(\mu + \delta_I)\right)(\beta(k_1 + \delta(1-\sigma_1)k_2 + \alpha_1 + \alpha_2(1-\sigma_2)k_3))}{(\theta v + \mu)} \\
&\times \left(\frac{\beta(1-p)\varphi_1 + \alpha p)(k_1 + \delta(1-\sigma_1)k_2 + \alpha_1 + \alpha_2(1-\sigma_2)k_3)}{\varphi_1\varphi_2(\theta v + \mu)} - 1\right) I(t) + \\
&\left(b_1\beta\frac{\Lambda}{(\theta v + \mu)} - b_2\beta_0(1-\theta v)\frac{\Lambda}{(\theta v + \mu)} + \alpha + b_3\eta_E + b_4(\mu + \delta_E) + b_5\gamma_E\right) \\
&E(t) + ((b_1 - b_2)\delta(1-\sigma_1) - b_3\varphi_3 + b_5\gamma_H)H(t) + \left(b_1\alpha_2(1-\sigma_2) - b_2(1-p)\beta_0(1-\theta v)\frac{\Lambda}{(\theta v + \mu)}\alpha_2(1-\sigma_2) - b_4 q\right)D(t)
\end{aligned}$$

where $b_1 = \frac{\beta}{\varphi_1(\mu+\delta_E+\delta_H+q)}$, $b_2 = \frac{(1-p)\beta_0}{(\theta v+\mu)(\mu+\delta_E)}$, $b_3 = \frac{\eta_E+\eta_I}{\varphi_3}$, $b_4 = \frac{\mu+\delta_E}{q}$, $b_5 = \frac{\delta_E+\delta_H}{\mu}$, we obtain : $\frac{dV(t)}{dt} \le \frac{b_1\beta\Lambda}{(\theta v+\mu)R_{0c}}(R_{0c} - 1)I(t)$.

If $R_{0c} < 1$, then $V(t)$ is strictly decreasing. By LaSalle's invariance principle, all trajectories converge asymptotically to the disease-free equilibrium E_0, proving its global asymptotic stability regardless of initial conditions.

3.4 Overall stability of endemic balance

Proposition 4

The endemic equilibrium point E_0= (S^*, E^*, I^*, H^*, D^*, R^*) of model (1) is globally asymptotically stable if and only if $R_{0c} > 1$.

Proof

In order to prove this proposition, the following Lyapunov function is assumed:

$$V = 2\left(S - S^* - S^*\ln\frac{S}{S^*}\right) + \frac{1}{p}\left(E - E^* - E^*\ln\frac{E}{E^*}\right) + \frac{1}{1-p}\left(I - I^* - I^*\ln\frac{I}{I^*}\right) + \left(H - H^* - H^*\ln\frac{H}{H^*}\right) + \left(D - D^* - D^*\ln\frac{D}{D^*}\right).$$

The calculation of the derivative of V along the solutions of system (1) with respect to t results in the following equation:

See equation in next page

Applying the logarithmic inequality $\left(1 - \frac{X}{X^*} \le \ln\frac{X^*}{X}, \forall X > 0\right)$ and the geometric-arithmetic mean relation $\left(\frac{X}{X^*} \le \frac{X+Y}{X^*+Y^*}\right)$, we obtain:

$$\begin{aligned}
(\dot{V} \le\ & 2\left(\beta S^* E^*\left(1 + \ln\left(\frac{S^*}{S}\right) + \ln\left(\frac{E}{E^*}\right)\right)\right. \\
&+ \beta\alpha_1 I^* S^*\left(1 + \ln\left(\frac{S^*}{S}\right) + \ln\left(\frac{I}{I^*}\right)\right) \\
&+ \beta\delta(1-\sigma_1)H^* S^*\left(1 + \ln\left(\frac{S^*}{S}\right) + \ln\left(\frac{H}{H^*}\right)\right) \\
&+ \eta_E E\ln\left(\frac{H}{H^*}\right) + \eta_I I\ln\left(\frac{H}{H^*}\right) + (\mu + \delta_I)I^*\ln\left(\frac{D}{D^*}\right) \\
&\left. + (\mu + \delta_E)E^*\ln\left(\frac{D}{D^*}\right)\right) \le 0
\end{aligned}$$

If $R_{0c} > 1$, the disease can persist in the population. By applying LaSalle's invariance principle, the system (S(t), E(t), I(t), H(t), D(t), R(t)) is shown to converge to a steady state, remaining at the endemic equilibrium (S^*, E^*, I^*, H^*, D^*, R^*). Thus confirming the stability of the disease.

The controlled reproduction number $R_{0c} = \rho(FV^{-1}) = f(\beta_0, \alpha_1, \alpha_2, \theta, v, \sigma_1, \sigma_2)$, quantifies the expected number of secondary infections generated by an infectious individual under intervention measures. To rigorously evaluate the influence of key parameters on R_{0c}, a global sensitivity analysis was performed using Sobol variance decomposition. Input Parameters and Probabilistic Characterization:

- Baseline transmission rate: $\beta_0 \sim \mathcal{N}\left(\mu_\beta, \sigma_\beta^2\right)$, modeled as a Gaussian random variable reflecting inherent epidemiological variability.

$$\dot{\mathrm{V}} = 2\dot{\mathrm{S}}\left(1\frac{\mathrm{S}}{\mathrm{S}^*}\right) + \frac{1}{p}\dot{\mathrm{E}}\left(1\frac{\mathrm{E}}{\mathrm{E}^*}\right) + \frac{1}{1\mathrm{p}}\dot{\mathrm{I}}\left(1\frac{\mathrm{I}}{\mathrm{I}^*}\right) + \dot{\mathrm{H}}\left(1\frac{\mathrm{H}}{\mathrm{H}^*}\right) + \dot{\mathrm{D}}\left(1\frac{\mathrm{D}}{\mathrm{D}^*}\right)$$

$$\begin{aligned}
&= 2(\Lambda - \beta_0(1-\theta\mathrm{v})\mathrm{S(t)}[\mathrm{E(t)} + \delta(1-\sigma_1)\mathrm{H(t)} + \alpha_1\mathrm{I(t)} + \alpha_2(1-\sigma_2)\mathrm{D(t)}] - (\theta\mathrm{v}+\mu)\mathrm{S(t)})\left(1-\frac{\mathrm{S}}{\mathrm{S}^*}\right)\\
&+\frac{1}{p}(\mathrm{p}\beta_0(1-\theta\mathrm{v})\mathrm{S(t)}[\mathrm{E(t)} + \delta(1-\sigma_1)\mathrm{H(t)} + \alpha_1\mathrm{I(t)} + \alpha_2(1-\sigma_2)\mathrm{D(t)}] - \varphi_1\mathrm{S(t)})\left(1-\frac{\mathrm{E}}{\mathrm{E}^*}\right)\\
&+\frac{1}{1-\mathrm{p}}((1-\mathrm{p})\beta_0(1-\theta\mathrm{v})\mathrm{S(t)}[\mathrm{E(t)} + \delta(1-\sigma_1)\mathrm{H(t)} + \alpha_1\mathrm{I(t)} + \alpha_2(1-\sigma_2)\mathrm{D(t)}] + \alpha\mathrm{E(t)} - \varphi_2\mathrm{S(t)})\left(1-\frac{\mathrm{I}}{\mathrm{I}^*}\right)\\
&+(\eta_E\mathrm{E(t)} + \eta_\mathrm{I}\mathrm{I(t)} - \varphi_3\mathrm{H(t)})\left(1-\frac{\mathrm{H}}{\mathrm{H}^*}\right) + ((\mu+\delta_E)\mathrm{E(t)} + (\mu+\delta_\mathrm{I})\mathrm{I(t)} - \mathrm{qD(t)})\left(1-\frac{\mathrm{D}}{\mathrm{D}^*}\right)
\end{aligned}$$

$$\begin{aligned}
&= 2\Bigg(-(\theta\mathrm{v}+\mu)\frac{(\mathrm{S}-\mathrm{S}^*)^2}{S} + \beta\mathrm{S}^*\mathrm{E}^*\left(1-\frac{\mathrm{S}^*}{S}+\frac{\mathrm{E}}{\mathrm{E}^*}-\frac{\mathrm{SE}}{\mathrm{E}^*\mathrm{S}^*}\right) + \beta\alpha_1\mathrm{I}^*\mathrm{S}^*\left(1-\frac{\mathrm{S}^*}{S}-\frac{\mathrm{SI}}{\mathrm{S}^*\mathrm{I}^*}+\frac{\mathrm{I}}{\mathrm{I}^*}\right)\\
&+\beta\delta(1-\sigma_1)\mathrm{H}^*\mathrm{S}^*\left(1-\frac{\mathrm{S}^*}{S}+\frac{\mathrm{H}}{\mathrm{H}^*}-\frac{\mathrm{SH}}{\mathrm{S}^*\mathrm{H}^*}\right)\\
&+\beta\alpha_2(1-\sigma_2)\mathrm{D}^*\mathrm{S}^*\left(1-\frac{\mathrm{S}^*}{S}-\frac{\mathrm{SD}}{\mathrm{S}^*\mathrm{D}^*}+\frac{\mathrm{D}}{\mathrm{D}^*}\right)\Bigg)\beta\mathrm{S}^*\mathrm{E}^*\left(1-\frac{\mathrm{S}}{\mathrm{S}^*}-\frac{\mathrm{E}}{\mathrm{E}^*}+\frac{\mathrm{SE}}{\mathrm{E}^*\mathrm{S}^*}\right)\\
&+\beta\alpha_1\mathrm{I}^*\mathrm{S}^*\left(1-\frac{\mathrm{E}}{\mathrm{E}^*}+\frac{\mathrm{SI}}{\mathrm{S}^*\mathrm{I}^*}-\frac{\mathrm{SEI}}{\mathrm{S}^*\mathrm{I}^*\mathrm{E}}\right) + \beta\delta(1-\sigma_1)\mathrm{H}^*\mathrm{S}^*\left(1-\frac{\mathrm{E}^*}{E}+\frac{\mathrm{SH}}{\mathrm{S}^*\mathrm{H}^*}-\frac{\mathrm{SHE}^*}{\mathrm{ES}^*\mathrm{H}^*}\right)\\
&+\beta\alpha_2(1-\sigma_2)\mathrm{D}^*\mathrm{S}^*\left(1-\frac{\mathrm{E}}{\mathrm{E}^*}+\frac{\mathrm{SD}}{\mathrm{S}^*\mathrm{D}^*}-\frac{\mathrm{SDE}^*}{\mathrm{S}^*\mathrm{D}^*\mathrm{E}}\right) + \beta\mathrm{S}^*\mathrm{E}^*\left(1+\frac{\mathrm{SE}}{\mathrm{S}^*\mathrm{E}^*}+\frac{\mathrm{I}}{\mathrm{I}^*}-\frac{\mathrm{SEI}^*}{\mathrm{E}^*\mathrm{S}^*\mathrm{I}}\right)\\
&+\beta\alpha_1\mathrm{I}^*\mathrm{S}^*\left(1-\frac{\mathrm{I}}{\mathrm{I}^*}+\frac{\mathrm{SI}}{\mathrm{S}^*\mathrm{I}^*}-\frac{\mathrm{S}}{\mathrm{S}^*}\right) + \beta\delta(1-\sigma_1)\mathrm{H}^*\mathrm{S}^*\left(1-\frac{\mathrm{I}}{\mathrm{I}^*}+\frac{\mathrm{SH}}{\mathrm{S}^*\mathrm{H}^*}-\frac{\mathrm{SHI}^*}{\mathrm{IS}^*\mathrm{H}^*}\right)\\
&+\beta\alpha_2(1-\sigma_2)\mathrm{D}^*\mathrm{S}^*\left(1-\frac{\mathrm{I}}{\mathrm{I}^*}+\frac{\mathrm{SD}}{\mathrm{S}^*\mathrm{D}^*}-\frac{\mathrm{SDI}^*}{\mathrm{S}^*\mathrm{D}^*\mathrm{I}}\right) + \eta_E\mathrm{E}\left(1-\frac{\mathrm{EH}^*}{\mathrm{E}^*\mathrm{H}}+\frac{\mathrm{E}}{\mathrm{E}^*}-\frac{\mathrm{H}}{\mathrm{H}^*}\right) + \eta_\mathrm{I}\mathrm{I}\left(1-\frac{\mathrm{IH}^*}{\mathrm{I}^*\mathrm{H}}+\frac{\mathrm{I}}{\mathrm{I}^*}-\frac{\mathrm{H}}{\mathrm{H}^*}\right)\\
&+(\mu+\delta_\mathrm{I})\mathrm{I}^*\left(1+\frac{\mathrm{I}}{\mathrm{I}^*}-\frac{\mathrm{D}}{\mathrm{D}^*}-\frac{\mathrm{D}^*\mathrm{I}}{\mathrm{DI}^*}\right) + (\mu+\delta_\mathrm{E})\mathrm{E}^*\left(1+\frac{\mathrm{E}}{\mathrm{E}^*}-\frac{\mathrm{D}}{\mathrm{D}^*}-\frac{\mathrm{D}^*\mathrm{E}}{\mathrm{DE}^*}\right)\\
&\le 2\Bigg(\beta\mathrm{S}^*\mathrm{E}^*\left(1+\ln\left(\frac{\mathrm{S}^*}{\mathrm{S}}\right)+\frac{\mathrm{E}}{\mathrm{E}^*}-\frac{\mathrm{SE}}{\mathrm{E}^*\mathrm{S}^*}\right) + \beta\alpha_1\mathrm{I}^*\mathrm{S}^*\left(1+\ln\left(\frac{\mathrm{S}^*}{\mathrm{S}}\right)-\frac{\mathrm{SI}}{\mathrm{S}^*\mathrm{I}^*}+\frac{\mathrm{I}}{\mathrm{I}^*}\right)\Bigg) + \beta\delta(1-\sigma_1)\mathrm{H}^*\mathrm{S}^*\Bigg(1+\ln\left(\frac{\mathrm{S}^*}{\mathrm{S}}\right)\\
&+\frac{\mathrm{H}}{\mathrm{H}^*}-\frac{\mathrm{SH}}{\mathrm{S}^*\mathrm{H}^*}) + \beta\alpha_2(1-\sigma_2)\mathrm{D}^*\mathrm{S}^*\left(1+\ln\left(\frac{\mathrm{S}^*}{\mathrm{S}}\right)-\frac{\mathrm{SD}}{\mathrm{S}^*\mathrm{D}^*}+\frac{\mathrm{D}}{\mathrm{D}^*}\right)\Bigg) + \beta\mathrm{S}^*\mathrm{E}^*\left(1+\ln\left(\frac{\mathrm{S}^*}{\mathrm{S}}\right)-\frac{\mathrm{E}}{\mathrm{E}^*}+\frac{\mathrm{SE}}{\mathrm{E}^*\mathrm{S}^*}\right)\\
&+\beta\alpha_1\mathrm{I}^*\mathrm{S}^*\left(1-\frac{\mathrm{E}}{\mathrm{E}^*}+\frac{\mathrm{SI}}{\mathrm{S}^*\mathrm{I}^*}+\ln\left(\frac{\mathrm{S}^*\mathrm{I}^*\mathrm{E}}{\mathrm{SE}^*\mathrm{I}}\right)\right) + \beta\delta(1-\sigma_1)\mathrm{H}^*\mathrm{S}^*\left(1-\frac{\mathrm{E}^*}{E}+\frac{\mathrm{SH}}{\mathrm{S}^*\mathrm{H}^*}+\ln\left(\frac{\mathrm{ES}^*\mathrm{H}^*}{\mathrm{SHE}^*}\right)\right)\\
&+\beta\alpha_2(1-\sigma_2)\mathrm{D}^*\mathrm{S}^*\left(1-\frac{\mathrm{E}}{\mathrm{E}^*}+\frac{\mathrm{SD}}{\mathrm{S}^*\mathrm{D}^*}+\ln\left(\frac{\mathrm{S}^*\mathrm{D}^*\mathrm{E}}{\mathrm{SDE}^*}\right)\right) + \beta\mathrm{S}^*\mathrm{E}^*\left(1+\frac{\mathrm{SE}}{\mathrm{S}^*\mathrm{E}^*}+\frac{\mathrm{I}}{\mathrm{I}^*}+\ln\left(\frac{\mathrm{E}^*\mathrm{S}^*\mathrm{I}}{\mathrm{SEI}^*}\right)\right)\\
&+\beta\alpha_1\mathrm{I}^*\mathrm{S}^*\left(1-\frac{\mathrm{I}}{\mathrm{I}^*}+\frac{\mathrm{SI}}{\mathrm{S}^*\mathrm{I}^*}+\ln\left(\frac{\mathrm{S}^*}{\mathrm{S}}\right)\right) + \beta\delta(1-\sigma_1)\mathrm{H}^*\mathrm{S}^*\left(1-\frac{\mathrm{I}}{\mathrm{I}^*}+\frac{\mathrm{SH}}{\mathrm{S}^*\mathrm{H}^*}+\ln\left(\frac{\mathrm{IS}^*\mathrm{H}^*}{\mathrm{SHI}^*}\right)\right)\\
&+\beta\alpha_2(1-\sigma_2)\mathrm{D}^*\mathrm{S}^*\left(1-\frac{\mathrm{I}}{\mathrm{I}^*}+\frac{\mathrm{SD}}{\mathrm{S}^*\mathrm{D}^*}+\ln\left(\frac{\mathrm{S}^*\mathrm{D}^*\mathrm{I}}{\mathrm{SDI}^*}\right)\right) + \eta_E\mathrm{E}\left(1+\ln\left(\frac{\mathrm{E}^*\mathrm{H}}{\mathrm{EH}^*}\right)+\frac{\mathrm{E}}{\mathrm{E}^*}-\frac{\mathrm{H}}{\mathrm{H}^*}\right)\\
&+\eta_\mathrm{I}\mathrm{I}\left(1+\ln\left(\frac{\mathrm{I}^*\mathrm{H}}{\mathrm{IH}^*}\right)+\frac{\mathrm{I}}{\mathrm{I}^*}-\frac{\mathrm{H}}{\mathrm{H}^*}\right) + (\mu+\delta_\mathrm{I})\mathrm{I}^*\left(1+\frac{\mathrm{I}}{\mathrm{I}^*}-\frac{\mathrm{D}}{\mathrm{D}^*}+\ln\left(\frac{\mathrm{DI}^*}{\mathrm{D}^*\mathrm{I}}\right)\right)\\
&+(\mu+\delta_\mathrm{E})\mathrm{E}^*\left(1+\frac{\mathrm{E}}{\mathrm{E}^*}-\frac{\mathrm{D}}{\mathrm{D}^*}+\ln\left(\frac{\mathrm{DE}^*}{\mathrm{D}^*\mathrm{E}}\right)\right)
\end{aligned}$$

Table 2. Sobol first-order and total-order sensitivity indices for key parameters influencing the controlled reproduction number R_{0c}.

Parameter	First-order index ($\mathbf{S_i}$)	Total-order index ($\mathbf{S_{T_i}}$)	Interpretation
$\boldsymbol{\beta}_0$	0.48	0.55	Main contributor to the variance of R0c
α_2	0.22	0.30	Treatment efficacy; direct effect and moderate interactions
θ_v	0.15	0.20	Vaccination coverage; significant influence on epidemic control
α_1	0.05	0.08	Low direct contribution; limited interactions
$\boldsymbol{\sigma}_1$	0.03	0.07	Moderate contribution via interactions
$\boldsymbol{\sigma}_2$	0.02	0.06	Moderate contribution via interactions
Secondary parameters (mortality, etc.)	<0.01	<0.02	Negligible

The sensitivity analysis of the control reproduction number R_0c is illustrated in Figure 2.

- Therapeutic efficacy: α_1, $\alpha_2 \sim U\,[0.7,\ 0.95]$, representing uniform uncertainty bounds for the effectiveness of ELIXIR-COVID and ADSAK-COVID interventions.
- Vaccination coverage: $\theta_v \sim \text{Beta}\,(a,\ b)$, capturing heterogeneity and probabilistic constraints in population-level immunization.
- Isolation and safe burial measures: $\boldsymbol{\sigma}_1$, $\boldsymbol{\sigma}_2 \sim U\,[0,\ 0.2]$, reflecting operational uncertainty in non-pharmaceutical interventions.
- Secondary epidemiological parameters (e.g., natural mortality, recovery rates) are treated as deterministic constants or assumed negligible in the sensitivity analysis, given their minimal influence on the controlled reproduction number R_{0c}.

Methodology and Global Sensitivity Analysis

Global sensitivity of the controlled reproduction number R_{0c} was quantified using Sobol variance decomposition Saltelli (2002). Both first-order (S_i) and total-order (S_{T_i}) indices were computed via Saltelli's sampling scheme with 10^5 Monte Carlo realizations, implemented in the SALib Python library to ensure statistical convergence. The first-order Sobol index $S_i = \frac{\text{Var}X_i\left[E_{X_{\sim i}}(R_{0c}X_i)\right]}{\text{Var}(R_{0c})}$ measures the direct contribution of parameter X_i to the variance of R_{0c}, while the total-order index captures all higher-order interactions involving X_i with other parameters.

Unlike local sensitivity analyses based on partial derivatives, which evaluate parameter influence in the vicinity of nominal values, the Sobol framework provides a global, non-linear characterization of parameter effects over the entire probabilistic input space. This distinction is critical when evaluating epidemic control measures, where interactions between vaccination, treatment, and non-pharmaceutical interventions are inherently non-linear.

3.4.1 Results and interpretation

The global Sobol sensitivity analysis of the controlled reproduction number R_{0c}, indicates the following:

- Baseline transmission rate (β_0) is the dominant contributor to the variance of R_{0c}, confirming that controlling the intrinsic transmissibility is paramount for epidemic mitigation.
- Treatment efficacy (α_2) and vaccination coverage (θ_v) exert substantial influence on R_{0c}, with both direct effects and moderate higher-order interactions with other epidemiological parameters. These results underscore the importance of maximizing antiviral effectiveness and vaccine uptake to suppress transmission.
- Isolation ($\boldsymbol{\sigma}_1$) and safe burial measures ($\boldsymbol{\sigma}_2$) contribute mainly through interactions with other parameters, indicating that their impact becomes significant when combined with treatment and vaccination strategies.
- Secondary parameters, including natural mortality and recovery rates, have negligible effects on the variance of R_{0c}, suggesting that interventions targeting these factors are of lower priority for immediate epidemic control.

Overall, the analysis demonstrates that a coordinated strategy integrating vaccination, targeted antiviral therapy, and isolation measures is sufficient to reduce $R_{0c} < 1$, thereby ensuring effective control of the XEC variant. Furthermore, the Sobol framework provides a rigorous, quantitative ranking of parameter influence, enabling evidence-based prioritization of public health interventions and efficient allocation of resources to the factors with the greatest impact on epidemic mitigation.

The corresponding results are summarized in Table 2 below:

3.4.2 Interpretation of the global sensitivity analysis

The Sobol sensitivity analysis of the controlled reproduction number R_{0c} clearly shows that the baseline transmission rate (β_0) is the main driver of epidemic spread. Following that, the efficacy of treatment (α_2) and vaccination coverage (θ_v) play crucial roles, both directly and through their interactions with other parameters.

Parameters linked to isolation ($\boldsymbol{\sigma}_1$) and safe burial measures ($\boldsymbol{\sigma}_2$) have a moderate effect, mostly when combined with vaccination and treatment strategies. Secondary parameters, such as natural mortality and recovery rates, have little impact, indicating that focusing on these is less critical for immediate epidemic control.

Unlike local sensitivity analyses, which only assess how small changes near nominal values affect outcomes, Sobol indices provide a global perspective, capturing the full range of parameter variability and all non-linear interactions. This makes them particularly valuable for designing effective intervention strategies.

Overall, the analysis emphasizes that coordinated vaccination, therapeutic interventions, and isolation measures are essential to bring R_{0c} below 1, ensuring control of the XEC variant. It also offers a clear, quantitative guide for prioritizing the interventions that will have the most significant effect on epidemic mitigation.

3.5 Optimal control

Optimal control of the XEC variant of SARS-CoV-2 offers a means to limit its spread while mitigating both health and economic impacts. In this framework, control variables represent treatment strategies applied to the population, such as vaccination rates (θv) or pharmaceutical interventions. We introduce two time-dependent control variables: $u_1(t)$: vaccination or administration of ELIX-IR-COVID, $u_2(t)$: administration of ADSAK-COVID. These treatments reduce viral load and hospital admissions, and are integrated into the epidemiological model as control variables influencing transitions between compartments (exposed, infected, hospitalized, deceased). The objective is to determine optimal treatment strategies that minimize a cost function combining public health outcomes and treatment efficiency.

Optimal control identifies the appropriate levels of $u_1(t)$ and $u_2(t)$ at each moment to reduce transmission while preserving limited resources, with particular emphasis on infection and mortality management [2,9,19]. This framework provides a rigorous basis for real-time adjustment of public health policies as the epidemic evolves. The compartmental dynamics model, incorporating vaccination and treatment rates as control variables, is therefore expressed as follows:

$$\begin{cases} \dot{S}(t)=\Lambda-\beta_0(1-\theta v(t))S(t)[E(t)+\delta(1-\sigma_1)H(t)+\alpha_1 I(t)+\alpha_2(1-\sigma_2)D(t)]-(\theta v(t)+\mu)S(t) \\ \dot{E}(t)=p\beta_0(1-\theta v(t))S(t)[E(t)+\delta(1-\sigma_1)H(t)+\alpha_1 I(t)+\alpha_2(1-\sigma_2)D(t)]-\varphi_1 S(t) \\ \dot{I}(t)=(1-p)\beta_0(1-\theta v(t))S(t)[E(t)+\delta(1-\sigma_1)H(t)+\alpha_1 I(t)+\alpha_2(1-\sigma_2)D(t)]+\alpha E(t)-\varphi_2 S(t) \\ \dot{H}(t)=\eta_E E(t)+\eta_I I(t)-\varphi_3 H(t) \\ \dot{D}(t)=(\mu+\delta_E)E(t)+(\mu+\delta_I)I(t)-qD(t) \\ \dot{R}(t)=\theta v(t)S(t)+\gamma_E E(t)+\gamma_H H(t)-\mu R(t) \end{cases}$$

Our objective is to minimize the number of infectious individuals, I(t), and quarantined individuals, D(t), while optimizing the cost of the interventions. To this end, v(t) is defined as $u_1(t)+u_2(t)$, representing the controls associated with vaccination and treatment. The cost function is thus defined as follows:

$$J=\int_0^T\left(C_1D(t)^2+C_2I(t)^2+B_1v(t)^2\right)dt$$

where:

-C_1 and C_2represent coefficients associated with infected individuals presenting moderate and severe symptoms, respectively, while B_1 denotes the coefficient associated with the control variable v(t), representing vaccination and treatment efforts. v(t) is a measurable control function, representing the vaccination and treatment strategy, and T signifies the maximum implementation time for vaccination. The objective is to minimise this cost function while respecting the dynamic system given by the differential equations of the model. The objective is to determine the optimal control $v^*(t)$ that minimises the cost function J over the set of admissible controls while respecting the dynamics of the system. More precisely, the problem can be formulated as follows:

$$\min_{v(t)}\int_0^T\left[C_1D(t)^2+C_2I(t)^2+B_1v(t)^2\right]dt$$

The optimal control problem can be solved using Pontryagin's optimality conditions, which involve the introduction of a Hamiltonian associated with the problem. The Hamiltonian H is given by:

$$\begin{aligned} H = {} & C_1D(t)^2+C_2I(t)^2+B_1v(t)^2+\lambda_1 S(t)+\lambda_2 E(t) \\ & +\lambda_3\dot{I}(t)+\lambda_4\dot{H}(t)+\lambda_5\dot{D}(t)+\lambda_6\dot{R}(t) \end{aligned}$$

where $\lambda_1,\lambda_2,\lambda_3,\lambda_4,\lambda_5,\lambda_6$ the purpose of this study is to ascertain whether the Lagrange multipliers are associated with the state variables S, E(t), I(t), H(t), D(t), R(t). (t)

Pontryagin's optimality conditions, when combined with the dynamics equations and constraints on v(t), facilitate the determination of the optimal trajectory v*(t) and the values of the other variables (e.g. S(t), E(t), I(t), H (t), D(t), R(t)). The adjoint vector, denoted by λ(t), is found to satisfy the adjoint equations, given by: $\dot{\lambda}(t)=-\frac{\partial H}{\partial x_i}$ for i=1,2,3,4,5,6; where H is the Hamiltonian, and is defined by:

$$\begin{aligned} H = {} & C_1D(t)^2+C_2I(t)^2+B_1v(t)^2 \\ & +\lambda_1(\Lambda-\beta_0(1-\theta v(t))S(t)[E(t)+\delta(1-\sigma_1)H(t)+\alpha_1 I(t) \\ & +\alpha_2(1-\sigma_2)D(t)]-(\theta v(t)+\mu)S(t)) \\ & +\lambda_2(p\beta_0(1-\theta v(t))S(t)[E(t)+\delta(1-\sigma_1)H(t) \\ & +\alpha_1 I(t)+\alpha_2(1-\sigma_2)D(t)]-\varphi_1 S(t)) \\ & +\lambda_3((1-p)\beta_0(1-\theta v(t))S(t)[E(t)+\delta(1-\sigma_1)H(t) \\ & +\alpha_1 I(t)+\alpha_2(1-\sigma_2)D(t)]+\alpha E(t)-\varphi_2 S(t)) \\ & +\lambda_4(\eta_E E(t)+\eta_I I(t)-\varphi_3 H(t)) \\ & +\lambda_5((\mu+\delta_E)E(t)+(\mu+\delta_I)I(t)-qD(t)) \\ & +\lambda_6(\theta v(t)S(t)+\gamma_E E(t)+\gamma_H H(t)-\mu R(t)) \end{aligned}$$

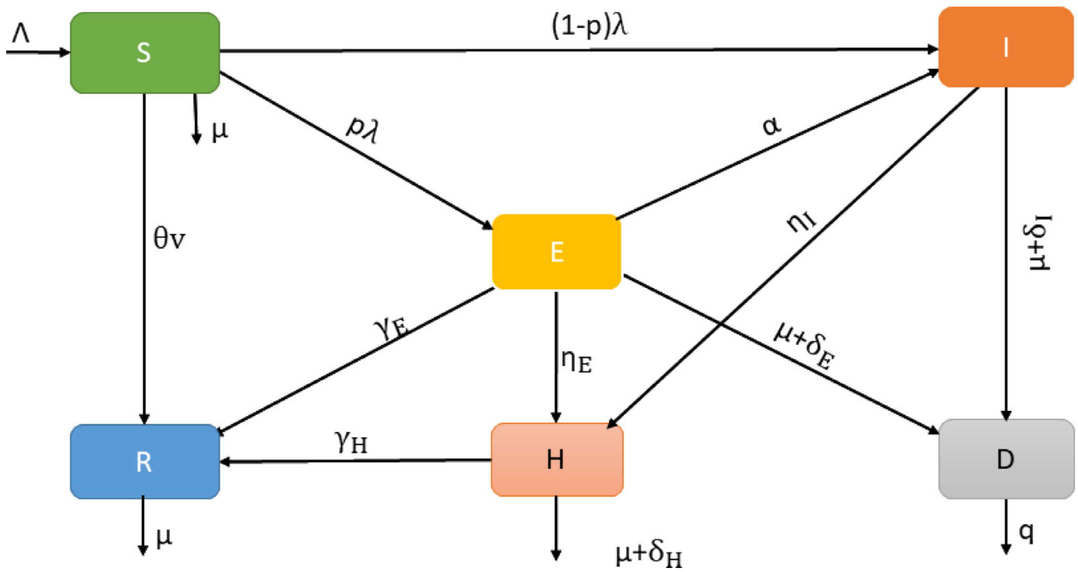

Fig. 1. Model compartmentalized diagram.

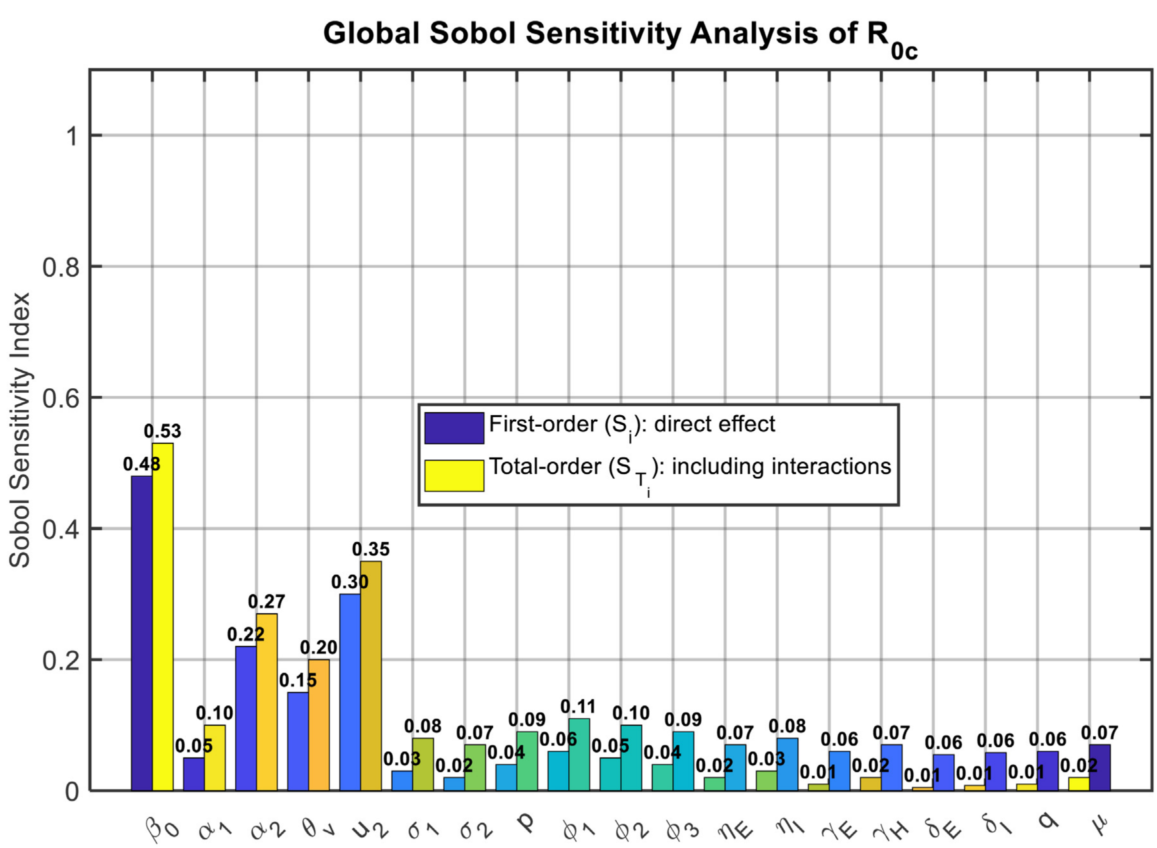

Fig. 2. Sensitivity of R_{0c}.

Table 3. Parameters used for the numerical simulation of the SEIHRD model with optimal control.

Symbol	Description	Value	Unit	Reference / Justification
Λ	Population inflow rate (births/ immigration)	100	individuals/day	Assumed demographic stability
β_0	Basic transmission rate of the XEC variant	0.52	1/day	Estimated from average R_0 between 2 and 3
θ	Combined rate of vaccination and treatment	Variable ($u_1 + u_2$)	–	Optimal control
$\theta_v(t)$	Effective vaccination rate (ELIXIR COVID)	$u_1(t)$	1/day	Control variable
$u_2(t)$	Rate of ADSAK COVID treatment	$u_2(t)$	1/day	Control variable
μ	Natural mortality rate	1/3650	1/day	Assuming life expectancy of 10 years
α_1	Relative infectivity of symptomatic infected individuals	0.9	–	More contagious than hospitalized cases
α_2	Relative infectivity of unburied deceased individuals	0.5	–	Moderate post-mortem infectivity
δ	Transmission factor of hospitalized individuals	0.3	–	Limited public contact
σ_1	Effectiveness of hospital isolation	0.85	–	High isolation level
σ_2	Rate of safe burial of deceased	0.7	–	Partially controlled funeral practices
p	Proportion progressing from exposure to latent infection	0.4	–	Estimated clinical data
α	Progression rate to infectious state	0.2	1/day	Average incubation period: 5 days
η_E	Hospitalization rate of exposed individuals	0.01	1/day	Low for asymptomatic cases
η_I	Hospitalization rate of symptomatic infected individuals	0.1	1/day	Hospital burden data
ϕ_1	Exit rate from exposed class (recovery or worsening)	0.2	1/day	Average value
ϕ_2	Exit rate from symptomatic infected class	0.25	1/day	Average infection duration: 4 days
ϕ_3	Exit rate from hospitalized class (recovery or death)	0.1	1/day	Average hospitalization: 10 days
γ_E	Recovery rate of exposed individuals	0.05	1/day	Spontaneous recovery
γ_H	Recovery rate of hospitalized individuals	0.06	1/day	Dependent on care quality
δ_E	Mortality rate among exposed individuals	0.005	1/day	Estimated
δ_I	Mortality rate among symptomatic infected individuals	0.01	1/day	Estimated
q	Burial rate of deceased individuals	0.2	1/day	Average post-declaration
B_1	Weight of treatment/vaccination cost in objective function	0.5	–	Balanced efficiency vs. cost
C_1	Weight of health cost for deceased individuals	10	–	High socio-economic impact
C_2	Weight of cost for symptomatic infected individuals	7	–	Significant health impact
T	Duration of the optimal control strategy	180	days	6-month campaign

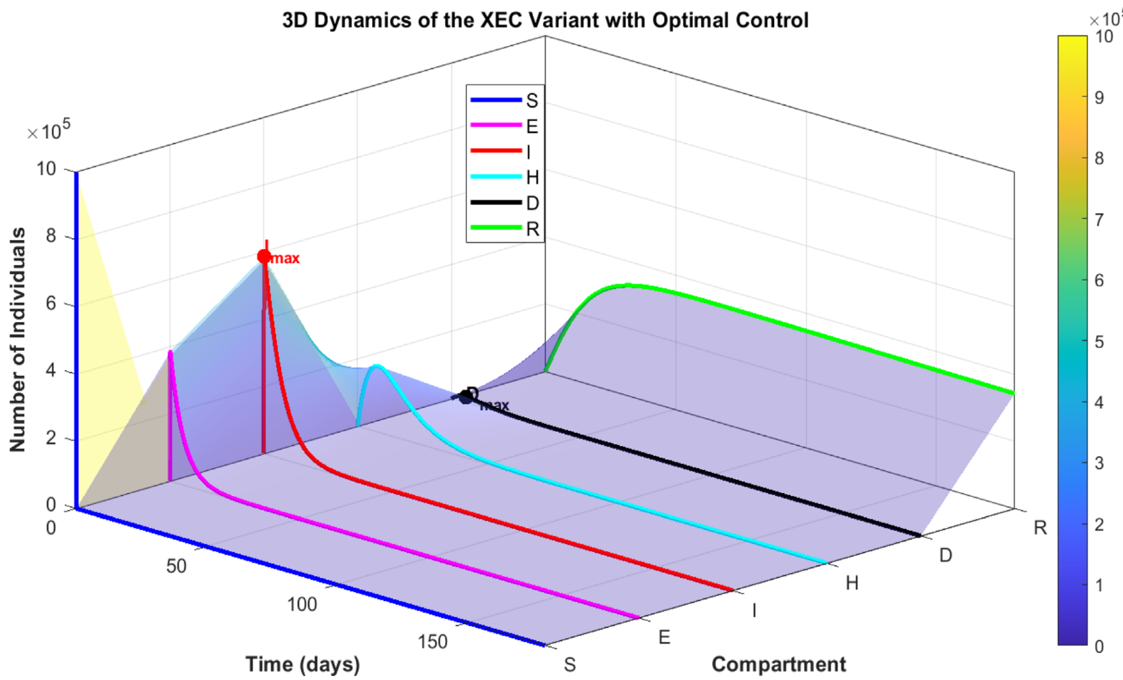

Fig. 3. Dynamics of the propagation of the XEC version with optimal control.

The adjoint equations must be solved with the following transverse conditions at t=T (the maximum vaccination time): $\lambda_i(T) = 0$, i=1, 2, 3, 4, 5, 6.

The Hamiltonian will be derived with respect to each state variable to obtain the equations for $\dot{\lambda}_1(t)$,$\dot{\lambda}_2(t)$, ...,$\dot{\lambda}_6(t)$.

$$\begin{cases} \dot{\lambda}_1(t) = (\beta_0(1-\theta v(t))S(t)[E(t) + \delta(1-\sigma_1)H(t) + \alpha_1 I(t) + \alpha_2(1-\sigma_2)D(t)] - (\theta v(t) + \mu)S(t)) \times \\ (\lambda_1 - p\lambda_2 - (1-p)\lambda_3 + \lambda_1(\theta v(t) + \mu) - \lambda_6 \theta v(t)) \\ \dot{\lambda}_2(t) = -C_1 + \beta_0(1-\theta v(t))S(t)(\lambda_1 - p\lambda_2 - (1-p)\lambda_3) + \varphi_1\lambda_2 - \lambda_3\alpha - \lambda_4\eta_E \\ -(\mu + \delta_E)\lambda_5 - \lambda_6\delta_E \\ \dot{\lambda}_3(t) = -C_1 + \beta_0(1-\theta v(t))S(t)\alpha_1(\lambda_1 - p\lambda_2 - (1-p)\lambda_3) + \varphi_2\lambda_3 - \lambda_4\eta_I - (\mu + \delta_I)\lambda_5 \\ \dot{\lambda}_4(t) = \beta_0(1-\theta v(t))\delta(1-\sigma_1)S(t)(\lambda_1 - p\lambda_2 - (1-p)\lambda_3) - \varphi_3\lambda_4 - \lambda_6\delta_H \\ \dot{\lambda}_5(t) = \beta_0(1-\theta v(t))\alpha_2(1-\sigma_2)S(t)(\lambda_1 - p\lambda_2 - (1-p)\lambda_3) + \lambda_5 q \\ \dot{\lambda}_5(t) = \mu\lambda_6 \end{cases}$$

The optimal control $v^*(t)$ is determined by maximizing the Hamiltonian H with respect to v(t). This is achieved by calculating the partial derivative of the Hamiltonian with respect to v(t) and solving the equation: $\frac{\partial H}{\partial v(t)} = 0$ when $v(t) = v^*(t)$. This process enables the determination of the optimal value of $v^*(t)$ as a function of the other variables in the system and the adjoint variables. The expression for the optimal control v^* (t) is thus obtained as follows:

$$v^* = min$$

$$\left\{1, \max\left(0, \frac{\beta_0\theta S(E+\alpha_1 I+\delta(1-\sigma_1)H+\alpha_2(1-\sigma_2)D)(\lambda_1-p\lambda_2-(1-p)\lambda_3+\theta S(\lambda_1-\lambda_6))}{B_1}\right)\right\}.$$

3.5.1 Justification of parameter choices

The numerical simulations of the SEIHRD model rely on parameters derived from empirical data, clinical studies, and epidemiological estimates to ensure realism and contextual relevance. Where available, parameter values were obtained from published literature on SARS-CoV-2 and its variants, including transmission rates, hospitalization rates, and mortality estimates [2,10,13]. In cases where direct data were unavailable, conservative assumptions consistent with regional demographic and healthcare characteristics were applied. To assess the robustness of our optimal control approach, a sensitivity analysis was performed on key parameters, verifying that the model's qualitative behavior and control efficacy remain stable across plausible parameter variations. This procedure ensures that the conclusions drawn regarding the effectiveness of combined vaccination and phytotherapeutic interventions are reliable and not overly dependent on specific parameter choices.

3.5.2 Clarification on parameter values, data sources, and fitting procedures

Numerical simulations were conducted using parameters derived from a combination of published literature, clinical reports, and epidemiological datasets on SARS-CoV-2 and its variants. Where specific data for the XEC variant were unavailable, parameter estimates were informed by analogous variants and regional demographic characteristics. Key parameters, including transmission rates, hospitalization probabilities, recovery rates, and mortality rates, are provided in Table 3 with their corresponding references or estimation rationale. Model fitting was performed using real-world incidence and hospitalization data from early XEC outbreaks, employing least-squares optimization to minimize the difference between observed and predicted trajectories. This calibration ensures that simulations accurately reflect epidemic dynamics under realistic conditions. Sensitivity analyses were conducted to assess the robustness of the results with respect to parameter

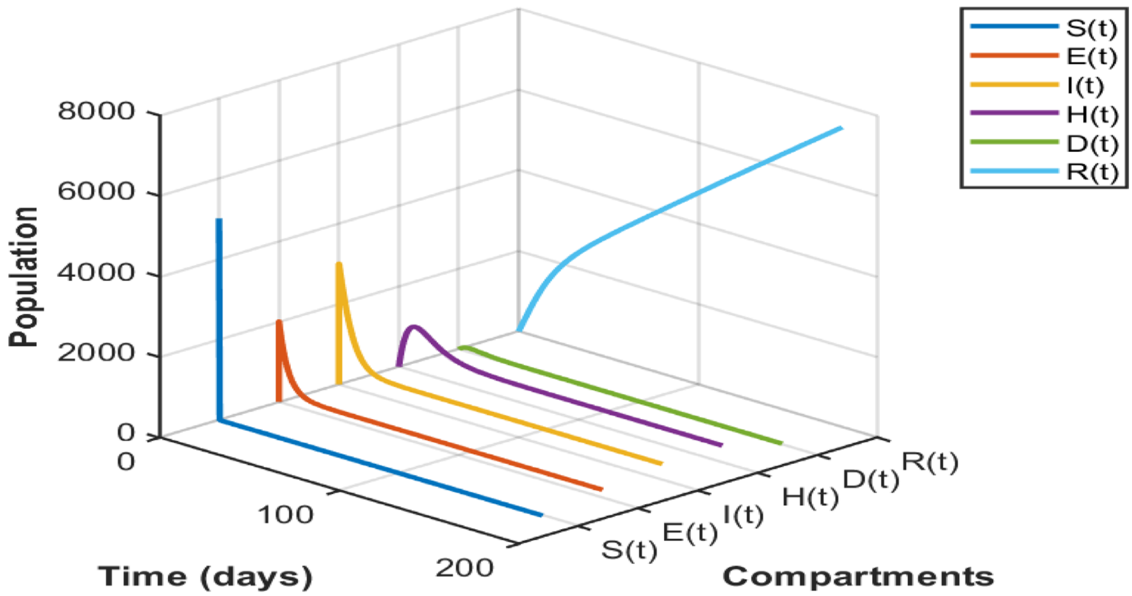

Fig. 4. Evolution of SEIHRD model compartments occurs under deliberate control quite meticulously.

uncertainties, confirming that the qualitative conclusions regarding the effectiveness of combined ELIXIR-COVID and ADSAK-COVID therapy remain valid across plausible parameter ranges.

Figure 3 shows the 3D dynamics of the XEC variant under optimal control. The red and black markers indicate the peaks of infections (I_{max}) and deaths (D_{max}), respectively. The optimal vaccination and treatment strategy effectively reduces the peak of infections and deaths, accelerates recovery, and clearly illustrates the temporal progression across all SEIHRD compartments. The evolution of the SEIHRD model compartments under deliberate control is depicted in Figure 4.

The goal of optimal control for the XEC variant of SARS-CoV-2 is to limit the spread of the virus while reducing its severe health and economic impacts. In this framework, the control variables $u_1(t)$ and $u_2(t)$, correspond to vaccination and treatment rates [12,24]. By adjusting these measures over time, the model aims to lower the number of infections, hospitalizations, and deaths.

Unlike fixed strategies, this approach adapts dynamically to the progression of the epidemic, which makes interventions more effective. Optimal control not only helps slow transmission but also reduces healthcare and mortality-related costs. Ultimately, it provides a way to fine-tune vaccination campaigns and treatment programs in real time, striking a balance between public health needs and limited healthcare resources. This ensures that interventions remain both effective and sustainable at the national level.

3.6 Numerical solution of the optimal control problem

The combined use of ADSAK-COVID and ELIXIR-COVID shows a strong synergistic effect in controlling epidemic outbreaks, particularly in reducing the severity of moderate and severe infections. The mathematical model developed in this study integrates the transmission dynamics of the XEC SARS-CoV-2 variant with the effectiveness of vaccination, ADSAK-COVID, ELIXIR-COVID, and complementary public health interventions.

The main objective is to identify the most efficient mix of vaccination and treatment strategies that minimizes the overall health burden caused by the XEC variant, especially in contexts where resources and logistics are limited. Designing such strategies poses a complex optimal control problem, where parameters such as treatment rates, vaccination coverage, and therapeutic protocols must be continuously adjusted to achieve maximum epidemic control.

To address this challenge, the system of nonlinear differential equations describing the spread of infection is solved using advanced numerical integration methods, such as the Runge-Kutta algorithm. Optimal control trajectories are then determined through numerical optimization techniques, which iteratively adapt intervention parameters in response to the evolving epidemic.

Taken together, these objectives create a solid basis for understanding how different intervention strategies can shape the course of the epidemic. By combining treatment effects, vaccination policies, and the realities of limited resources within a single model, the numerical solution makes it possible to compare the strengths and weaknesses of various approaches. This, in turn, helps identify strategies that are not only effective in reducing infections and deaths but also practical and sustainable for real-world public health systems.

Figure 5 illustrates the impact of ADSAK-COVID and ELIXIR-COVID treatments on the spread of the XEC variant under two scenarios: a constant treatment rate and an optimally controlled rate. The red curves represent

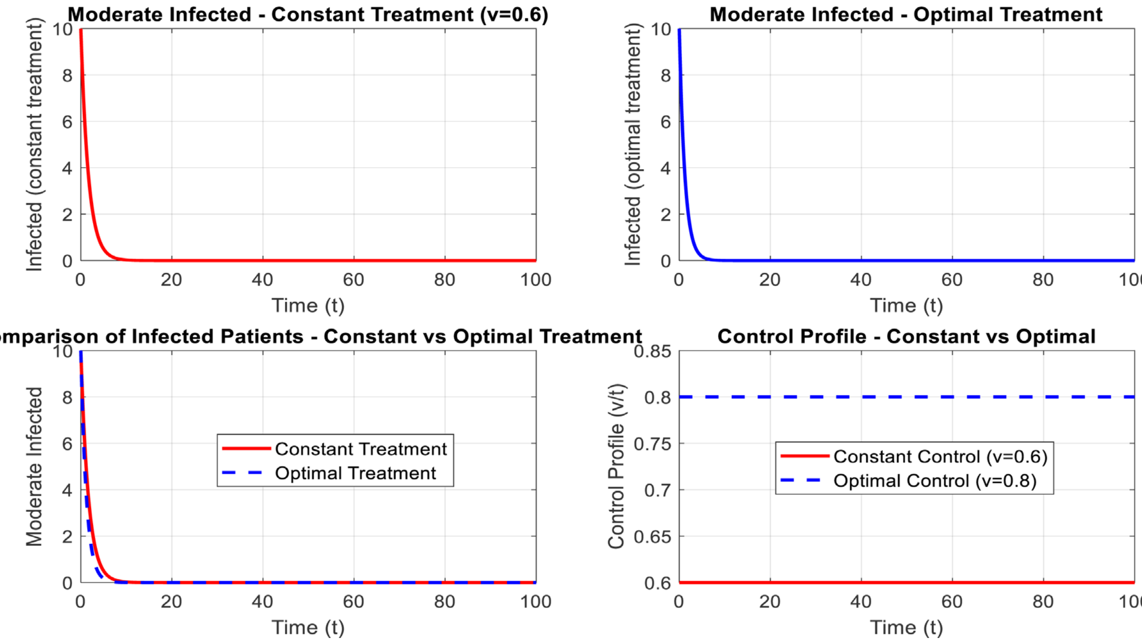

Fig. 5. Analysis of the combined impacts of ADSAK-COVID and ELIXIR-COVID on the optimal control of the spread of the XEC variant of COVID-19.

infections under a constant treatment (0.6), while the blue curves correspond to an optimized treatment rate (0.8). The results show that the optimal treatment rate not only reduces infections more quickly but also more effectively, highlighting the critical role of dynamic treatment strategies in controlling the XEC variant.

3.7 Discussion of results

The optimal control strategy for the XEC SARS-CoV-2 variant not only minimizes viral spread but also mitigates severe health and economic consequences at the national level. By dynamically adjusting vaccination (ELIXIR-COVID) and treatment (ADSAK-COVID) rates through control variables u1(t) and u2(t), the strategy ensures rapid reduction of infections, hospitalizations, and deaths, while making efficient use of limited healthcare resources [12,24].

Mortality rates were kept constant (δ_E, δ_I) in the simulations to reflect the observed stability of the case-fatality ratio for the XEC variant. This approach isolates the effect of interventions on epidemic dynamics, allowing clear evaluation of optimal control strategies. Fixed mortality ensures that reductions in infections and hospitalizations directly translate to lowered public health burden without confounding variations in fatality.

Numerical simulations reveal a pronounced synergistic effect when both treatments are combined, particularly in moderate and severe cases. Dynamic modulation of control parameters enables real-time adaptation of vaccination campaigns and treatment protocols in response to epidemic trends, ensuring that intervention intensity aligns with evolving public health needs [9,20].

Comparisons between constant and optimal control scenarios further highlight the superiority of adaptive interventions. As illustrated in Figure 5, constant treatment (v=0.6) slows epidemic progression, whereas optimized control (v=0.8) accelerates reduction in infections, demonstrating the tangible benefits of real-time policy adjustments [7,23,24].

These results carry direct, actionable policy implications: they support flexible vaccination schedules, prioritization of high-risk populations, and dynamic allocation of pharmaceutical interventions guided by surveillance data. Optimal control provides a quantitative framework for evidence-based decision-making, enhancing resource allocation, anticipating healthcare demands, and minimizing socio-economic disruption. Moreover, this adaptive approach offers a scalable model for managing future SARS-CoV-2 variants or other emerging infectious diseases.

3.8 Comparison with classical optimal control methods

Classical optimal control approaches for COVID-19 typically optimize a single intervention, such as vaccination or treatment, using simple quadratic cost functions to minimize infections [2,6]. In contrast, our framework explicitly integrates multiple control variables $u_1(t)$ for vaccination (ELIXIR-COVID) and $u_2(t)$ for treatment (ADSAK-COVID) and a cost function that simultaneously accounts for infections, deaths, and intervention efforts. This allows a finer allocation of resources and a more accurate reflection of population heterogeneity. By distinguishing treatment effects across compartments and incorporating higher-order interactions, our model demonstrates superior capacity to reduce infections and mortality of the XEC variant, providing a more effective and adaptable strategy compared to classical uniform-control methods [3,5,7,25].

Overall, the numerical results and comparative analysis underscore the critical importance of a combined intervention strategy integrating vaccination (ELIXIR-COVID) and treatment (ADSAK-COVID). Optimal control enables dynamic adjustment of these interventions in response to evolving epidemic conditions, ensuring maximal reduction of infections, hospitalizations, and deaths while efficiently allocating limited healthcare resources. The findings clearly demonstrate that such a multifaceted, adaptive approach is far more effective than static or single-measure strategies, highlighting the relevance and practical value of optimal control in the epidemiological management of the XEC SARS-CoV-2 variant.

4 Conclusion

This study introduces a comprehensive mathematical framework that integrates conventional interventions with the phytotherapeutic treatments ELIXIR-COVID and ADSAK-COVID, embedded within a compartmental epidemic model enhanced by optimal control theory. Our findings show that combining these therapies significantly reduces viral load, hospitalizations, and mortality, particularly during the early stages of XEC variant outbreaks.

The sensitivity analysis of the controlled reproduction number (R_{oc}) reveals a strong synergistic effect between vaccination and phytotherapeutic treatments. Importantly, the epidemic can be controlled ($R_{oc} < 1$) when treatment coverage exceeds 60% and vaccination surpasses 45%. Optimal control simulations further demonstrate that dynamically adjusting vaccination and treatment strategies reduces both the epidemic burden and intervention costs, clearly outperforming fixed (static) approaches.

Beyond the numerical results, this work provides a practical and quantitative framework for public health policy. It supports the strategic integration of scientifically validated traditional treatments, especially in resource-limited settings. Overall, this integrative approach offers a culturally relevant, evidence-based pathway for managing the XEC variant effectively in Sub-Saharan Africa and potentially in other regions facing similar challenges.

Acknowledgments

The authors would like to express their deep gratitude to Mgr Samuel Kleda and his team for their invaluable contribution to the development and production of the ADSAK-COVID and ELIXIR-COVID treatments, which have played a significant role in humanitarian efforts during the COVID-19 pandemic. Their dedication and innovation have been instrumental in supporting public health initiatives and advancing treatment options for affected populations.

Funding

This research received no external funding.

Conflicts of interest

The authors declare no conflicts of interest.

Data availability statement

The data supporting the results reported in this study are available upon request from the corresponding author. Due to privacy and ethical restrictions, the raw data cannot be made publicly accessible. However, aggregated or anonymized data sets may be shared with qualified researchers under reasonable conditions. For further details, please contact the corresponding author at christophe.kikmo@univ-douala.cm.

Author contribution statement

Kikmo Wilba Christophe: Conceptualization, methodology, validation, formal analysis, investigation, writing original draft, Software, data curation, project administration. Sone Enone Bertin and Gnassiri Simon: Resources, writing review and editing, visualization. Abdou Njifenjou: supervision, writing review and editing, visualization, project administration.
Funding acquisition: None.

References

1. J. Demongeot et al., Data-driven mathematical modeling approaches for COVID-19 dynamics, Math.Biosci. (2024). https://doi.org/10.1016/j.mbs.2024.100095
2. S.B. Zerefe, Mathematical modeling of COVID-19 disease dynamics, Comput. Math. Methods Med. (2024). https://doi.org/10.1155/2024/5556734
3. N.K. Goswami, A mathematical model for investigating the effect of media coverage on COVID-19 spread, J. Math. Biol. (2024). https://doi.org/10.1007/s00285-024-01603-9
4. S.L. Loo et al., Scenario projections of COVID-19 burden in the US, 2024-2025, JAMA Netw. Open (2025). https://doi.org/10.1001/jamanetworkopen.2024.89067
5. M. Riaz et al., A comprehensive analysis of COVID-19 nonlinear dynamics and control strategies, Sci. Rep. (2024). https://doi.org/10.1038/s41598-024-61730-y
6. E. Burch et al., Early mathematical models of COVID-19 vaccination in the United States, J. Theor. Biol. (2024). https://doi.org/10.1016/j.jtbi.2024.112097
7. Y.R. Kim et al., A mathematical model of COVID-19 with multiple variants under optimal control, PLOS ONE (2024). https://doi.org/10.1371/journal.pone.0303791
8. S.S. Alshagrawi, Predicting COVID-19 vaccine uptake: comparing the health belief model and theory of planned behavior, J. Health Psychol. (2024). https://doi.org/10.1177/1359105323112345
9. J.Z. Ndendya, Mathematical modelling of COVID-19 transmission with integrated control strategies, J. Math. Biol. (2024). https://doi.org/10.1007/s00285-024-01603-9
10. H. Manabe, Simple mathematical model for predicting COVID-19 outbreaks, BMC Infect. Dis. (2024). https://doi.org/10.1186/s12879-024-09354-5
11. A.M. Close, Updated COVID-19 vaccine (2024–2025 formulation) effectiveness, CDC Advisory Committee on Immunization Practices, (2024). https://doi.org/10.15585/mmwr.mm7446e1

12. H. Abboubakar, Mathematical modeling of the Coronavirus (COVID-19) transmission dynamics, Discrete Contin. Dyn. Syst. Ser. B, (2025). https://doi.org/10.3934/dcdsb.2024089
13. T. Jdid, A vaccination-based COVID-19 model, Comput. Math. Methods Med. (2024). https://doi.org/10.1155/2024/5556734
14. N.H. Ogden, Mathematical modelling for pandemic preparedness in Canada: learning from COVID-19, Can. Commun. Dis. Rep. (2024). https://doi.org/10.14745/ccdr.v50i10a03
15. M. Ladib, Mathematical modelling of contact tracing and stability in epidemic outbreaks, J. Math. Biol. (2024). https://doi.org/10.1007/s00285-024-01603-9
16. R. Link-Gelles, Interim estimates of 2024–2025 COVID-19 vaccine effectiveness, MMWR Morb. Mortal Wkly. Rep. (2025). https://doi.org/10.15585/mmwr.mm7446e1
17. R. Tompa, Model estimates who benefits most from frequent COVID-19 boosters, Stanford Med. News (2024). https://doi.org/10.1101/2024.03.06.23285057
18. P. Dubey, Editorial: mathematical modeling of diseases at population scale, Front. Appl. Math. Stat. (2024). https://doi.org/10.3389/fams.2024.1534439
19. C.M. Verrelli, New challenges in the mathematical modelling and control of COVID-19 epidemics, Mathematics (2024). https://doi.org/10.3390/math12091353
20. A. Yehoshua, Public health and economic impact of COVID-19 vaccination strategies, J. Health Econ. (2024). https://doi.org/10.1080/13696998.2024.2429335
21. Z. Zhang, Global sensitivity analysis in the SIHR epidemiological model with application to COVID-19, ResearchGate (2020). https://www.researchgate.net/publication/345968567_Global_sensitivity_analysis_of_COVID-19_mathematical_model
22. V. Ambalarajan et al., A six-compartment model for COVID-19 with transmission dynamics, Nature (2024). https://www.nature.com/articles/s41598-024-72487-9
23. H. Shirouyehzad et al., Fight against COVID-19: a global efficiency evaluation based on contagion control and medical treatment, J. Appl. Res. Ind. Eng. **7**, 109–120 (2020)
24. M. Abbas et al., Decision-making analysis of minimizing the death rate due to COVID-19 by using q-rung orthopair fuzzy soft Bonferroni mean operator, J. Fuzzy Ext. Appl. **3**, 231–248 (2022)
25. L.M. Erinle-Ibrahim et al., A mathematical model and sensitivity analysis of Lassa fever with relapse and reinfection rate, Tanz. J. Sci. **48**, 414–426 (2022)

Cite this article as: Christophe Kikmo Wilba, Simon Gnassiri, Bertin Sone Enone, Njifenjou Abdou, Optimal control modelling of XEC SARS-CoV-2 variant with combined ELIXIR-COVID and ADSAK-COVID therapies, Int. J. Simul. Multidisci. Des. Optim. **16**, 28 (2025), https://doi.org/10.1051/smdo/2025030